Journal of Applied Polymer Science

Thermal and Rheological Properties of Polyethylene Blends with Bimodal Molecular Weight Distribution

Hong-Wang Shen, Bang-Hu Xie, Wei Yang, Ming-Bo Yang

College of Polymer Science and Engineering, State Key Laboratory of Polymer Materials Engineering, Sichuan University, Chengdu, Sichuan 610065, People's Republic of China

Correspondence to: B.-H. Xie (E-mail: xiebangh@tom.com)

ABSTRACT: Polyethylene blends with bimodal molecular weight distribution were prepared by blending a high molecular weight polyethylene and a low molecular weight polyethylene in different ratios in xylene solution. The blends and their components were characterized by the high temperature gel permeation chromatograph (GPC), different scanning calorimetry (DSC), and small amplitude oscillatory shear experiments. The results showed that the dependence of zero-shear viscosity (η_0) on molecular weight followed a power law equation with an exponent of 3.3. The correlations between characteristic frequency (ω_0) and polydispersity index, and between dynamic cross-point (G_x) and polydispersity index were established. The complex viscosity (η^*) at different frequencies followed the log-additivity rule, and the Han-plots were independent of component and temperature, which indicated that the HMW/LMW blends were miscible in the melt state. Moreover, the thermal properties were very similar to a single component system, suggesting that the blends were miscible in the crystalline state. © 2013 Wiley Periodicals, Inc. J. Appl. Polym. Sci. 000: 000–000, 2013

KEYWORDS: bimodal polyethylene; dynamic rheology; solution blending; miscibility

Received 17 September 2012; accepted 19 November 2012; published online
DOI: 10.1002/app.38850

INTRODUCTION

There is no doubt that polyethylene (PE) is one of the most important plastic materials with utilities in industry, agriculture and other fields. The properties of polyolefine mainly depend on the polymer structure, especially the molecular weight and molecular weight distribution (MWD).[1–4] Generally, higher molecular weight will bring about better final mechanical properties, but it also gives rise to high melt viscosity and poor processability, which limits the application of PE. Recently, polyethylene with bimodal molecular weight distribution (defined as bimodal PE) can resolve the conflict between mechanical properties and processability very well.

Because of their good processing characteristics and excellent mechanical properties, bimodal PE arouses the researchers' interest quickly. This bimodal PE is composed of low molecular weight PE fraction and high molecular weight PE fraction. In bimodal PE, the low molecular weight fraction guarantees the stiffness and creep resistance in crystalline state, and reduces the melt viscosity during processing. Meanwhile, the high molecular weight fraction acts as the tie molecular that connect the crystal lamella mainly formed by the low molecular weight fraction, and so the impact strength and stress cracking resistance are enhanced. The combined action of these two fractions results in a good balance between mechanical properties and processability.[5–7] At present, bimodal PE is produced through two methods in industry: the reactor in series configuration and the single reactor with dual site catalysts.[8–11] And yet for all that, both of the two methods are complex and expensive, and it is difficult to produce a series of bimodal PE with continuously variable MWD. Essentially bimodal PE can be considered as a blend of two PE components with different molecular weight and MWD. Therefore, a melt blending is better suited to prepare a series of bimodal PE with continuously variable MWD in laboratory, but the bad mixed effect may seriously affect the research results. So a solution blending has been applied and proved to work well in PE blending for research purpose because of the most intimate mixing at the molecular level.[12–15]

At present, there are many reports about the effect of molecular weight, MWD and comonomer on the properties of polyolefin.[1,5,16–26] But for bimodal PE, the research mainly focuses on the synthetic technology and performance comparison to unimodal PE, while the study about the effect of bimodal MWD characteristic on the properties is relatively rare.[14,15]

In our previous works,[27,28] the bimodal MWD characteristic was regulated by blending bimodal PE with unimodal PE, but the range of regulation was very limited. In this paper, two

Table I. Molecular Characteristics of the Blends and Their Components

HMW/LMW	M_w (kg/mol)	M_n (kg/mol)	M_w/M_n
100/0	761.8	71.76	10.6
90/10	656.5	29.87	22.2
80/20	598.6	21.14	27.6
70/30	525.8	16.44	31.0
60/40	453.4	13.50	32.3
0/100	76.7	15.70	4.9

unimodal PE components with great difference in molecular weight were blended to prepare a series of bimodal PE blends with wide range of MWD regulation, then the thermal and melt rheological properties of these bimodal PE blends were obtained to examine their crystallization, viscosity, modulus, and miscibility characteristics in detail.

EXPERIMENTAL

Materials and Sample Preparation

Two different HDPE components (trade marked as DMDY 1158 and 5000S) with unimodal MWD were used in this paper: DMDY 1158, regarded as the high molecular weight fraction (HMW), was supplied as powder from Qilu Petrochemical Company, China with M_w = 762 kg/mol, M_w/M_n = 10.6, density of 0.953 g/cm^3 and a melt flow rate of 0.04 g/10min (230°C, 5 kg). The low molecular weight fraction (LMW) was prepared from 5000S, supplied as pellets by Lanzhou Fushun Petrochemical Company, China with M_w = 373 kg/mol, M_w/M_n =4.30, density of 0.951 g/cm^3 and a melt flow rate of 0.950 g/10 min (190°C, 2.16 kg). The procedures were the following: the autoclave was preheated to the preset temperature (350°C), then HDPE was placed in the autoclave with ultra-high purity dry nitrogen for preventing oxidative degradation and was held at this temperature for 15 min, and then cooled down to 40°C within 20 min before retrieval. The more details of the autoclave and procedures have been described elsewhere.[29]

The polymer blends were prepared by a solution blending procedure to ensure that the two species were intimately mixed at the molecular level. The blending procedures were as follows: the mixture of HMW, LMW and 0.3 wt % antioxidant agent (Irganox 1010) was first dissolved in xylene to form a homogeneous solution, and 100 mL xylene were required for per gram of polymers. Then the mixture was heated slowly under vigorous stirring until the polymers were completely dissolved in xylene (the solution became transparent). After the solution was held at 130°C for 60 min with continuous stirring, the precipitation of the polymer blends was carried out by pouring the polymer solution into cold absolute ethyl alcohol (about six times the original volume of xylene in the polymer solution) under continuous stirring. Finally, the polymer blends slurry was filtered from the xylene and ethanol mixture and vacuum-dried at 80°C for 72 h. Control samples of the pure HMW and LMW were also prepared as reference materials using the same procedure as the blends. The compositions of HMW/LMW blends were summarized in Table I.

Microstructural Characterization

The average molecular weight and MWD of the HMW/LMW blends and their components were measured by the high temperature gel permeation chromatograph (Model PL-GPC 220 UK). It was carried out at 160°C with 1, 2, 4-trichlorobenzene (TCB) as a solvent. Four columns with pore size of 10^3, 10^4, 10^5, and 10^6 Å were calibrated with narrow MWD polystyrene sample.

Thermal Analysis

The HMW/LMW blends and their components were analyzed using a Q-20 DSC (TA Instruments) for crystallization and melting studies. Calibration for the temperature scan was performed using indium as the standard to ensure reliability of the data obtained. Sample disks of about 0.2 mm thickness were used to guarantee maximum contact of the sample with aluminum sample pan to minimize the thermal lag between samples and DSC furnace. The experiments were carried out with about 5–10 mg of samples sealed in aluminum pans under dry nitrogen. Samples were heated from 40 to 160°C at a rate of 40°C/min, and held at this temperature for 5 min to erase any previous thermal history. They were then cooled at a rate of 10°C/min to 40°C, and finally heated again from 40 to 160°C at 10°C/min. Both the exothermic and endothermic curves were recorded. All tests were repeated at least three times to evaluate the accuracy of the data. The cooling scans were analyzed for the crystallization temperature T_c, while the second heating scans were used to obtain the melting temperatures T_m. All these results were the average of three tests and their error bars were necessary.

Dynamic Rheological Measurements

The linear viscoelastic properties of the HMW/LMW blends and their components in the melt state were measured using the TA instruments AR2000ex rotational rheometer. The samples were compression molded into the disk of 25 mm in diameter and around 1.5 mm in thickness. The measurements were then run with 25 mm parallel plate geometry and 1 mm sample gap. Thermal stability of samples during the rheological testing was check by a time sweep, where the selected samples gave a stable G' signal for at least 20 min at 210°C. The dynamic viscoelastic properties were determined with frequency from 0.01 to 100 Hz, using strain values determined with a stress sweep to lie within the linear viscoelastic region. Measurements were carried out in nitrogen atmosphere at four different temperatures 150, 170, 190, and 210°C, and all of frequency sweeps were finished within 15 min.

RESULTS AND DISCUSSION

Figure 1 shows the MWD curves of the HMW/LMW blends and their components obtained by GPC analysis, and the detailed parameters are listed in Table I. As shown in Figure 1, both HMW and LMW have the unimodal MWD, and their peak positions are 5.31 and 4.36 on the X-axis, respectively. The LMW has a reasonably narrow and symmetrical MWD (M_w/M_n = 4.9), and the MWD of HMW is broader (M_w/M_n = 10.6), mainly due to tailing both in low molecular weight and high molecular weight regions. The peak height for HMW decreases

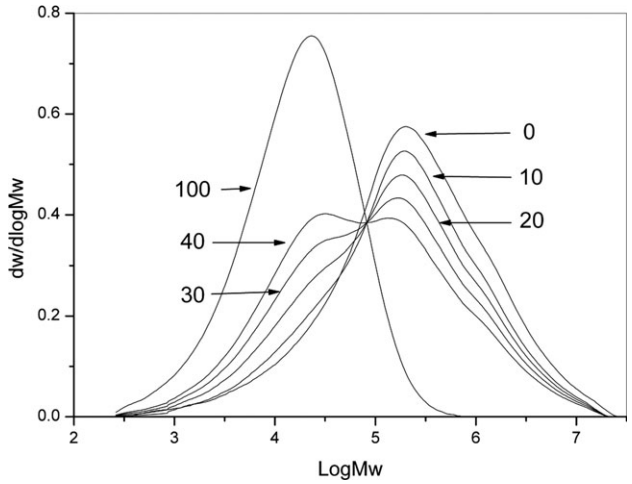

Figure 1. MWDs of HMW/LMW blends and their components (weight fraction of LMW in the blend indicated).

gradually with increasing in the content of LMW, and the other peak presents in low molecular weight region when the content of LMW is up to 20 wt %. The polydispersity index gradually increases from 10.6 of the HMW to 32.3 of the blend with 40 wt % LMW. The bimodal characteristic of HMW/LMW blends is seen as a MWD showing two distinct, partially overlapping peaks. Table I indicates that the molecular weight difference between HMW and LMW is about 10-fold. And also for these large differences in molecular weight, peak position, and polydispersity index of two PE components, the HMW/LMW blends show so distinct bimodal MWD.[30–32] Moreover, assuming that HMW and LMW have well dispersive effect, the weight-average molecular weight (M_w) of the blends should reflect the mixture of components. As shown in Figure 2, the measured M_w values of blends almost follow the connecting line between M_w values of components, indicative of the homogeneity of two components. Overall, the homogeneous bimodal PE blends can be successfully prepared by blending the HMW with LMW.

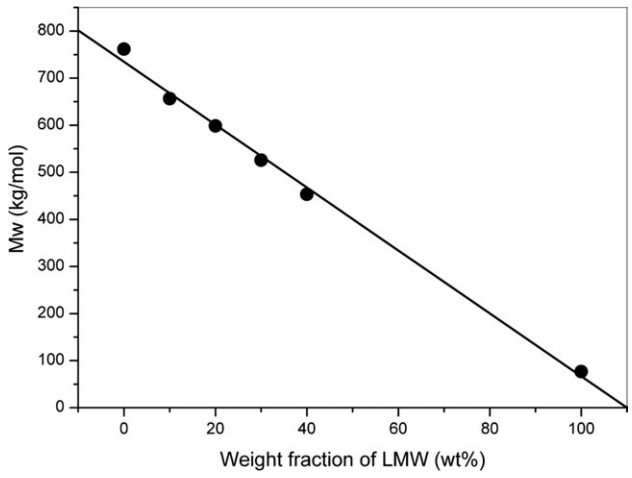

Figure 2. The component dependence of M_w for HMW/LMW blends (the solid line represent linear fitting of the measured data).

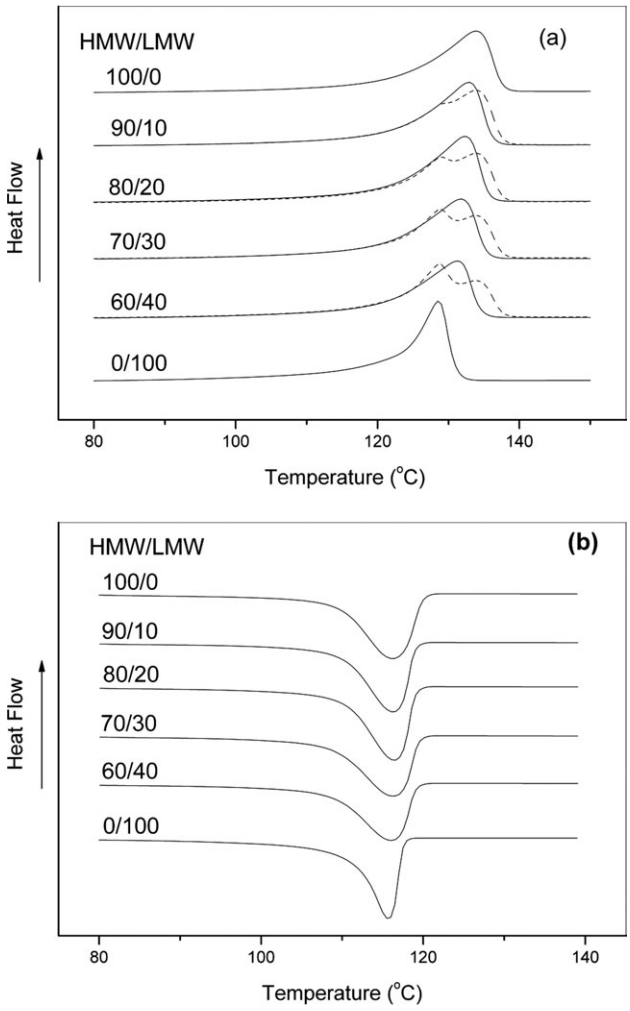

Figure 3. DSC scan curves of HMW/LMW blends and their components: (a) heating (solid lines represent the melt mixed blends and the dash lines represent the unmixed blends), (b) cooling.

Thermal Properties

The DSC melting and cooling scan curves of the HMW/LMW blends (mixed and "unmixed" blends) and their components are plotted in Figure 3(a,b), respectively. The scans corresponding to the "unmixed" blends were obtained by the weighted mathematical superposition of the corresponding pure components. As shown in these figures, the melting point of HMW is higher than that of LMW, due to the thicker lamellar formed by the longer molecular chains of HMW. The lower and broader melting peak for HMW is also observed, which can be explained by the broader range of lamellae thickness caused by the heterogeneous distribution of molecular chain length. Figure 3(a) shows that the "unmixed" blends exhibit two very clear melting endotherms (dash line), as opposed to the real mixed blends, which show only one endotherm at intermediate temperature with respect to the melting peaks of the pure components (solid line). In other words, if there are absolutely no contacts between the two pure polymers, the DSC will be able to differentiate the signal of the two components.

Only one melting and crystallization temperature peak were observed for all compositions of the blend systems, and the

Applied Polymer SCIENCE

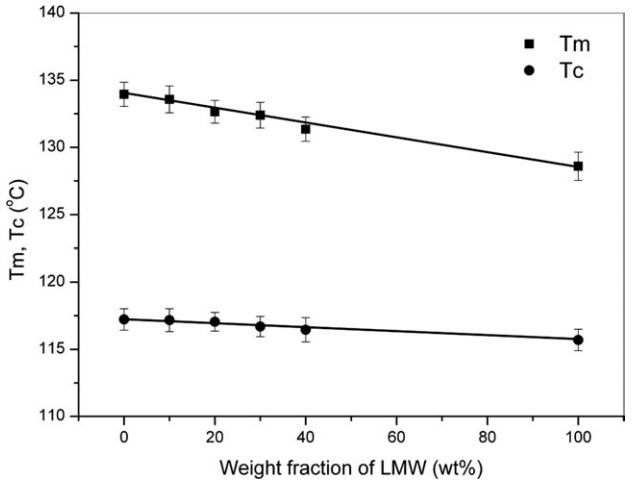

Figure 4. Component dependence of T_m and T_c for HMW/LMW blends.

component dependence of the melting point (T_m) and the crystallization temperature (T_c) almost follow linear relationship (Figure 4), indicative of cocrystallization of HMW and LMW. When cocrystallization occurs, the thermal and physical properties of the blend system are intermediate with respect to individual components, a fact that may be considered as an indicator of miscibility.[33,34]

Rheological Properties

Small amplitude oscillatory shear experiments were carried out to determine the rheological characteristics of the HMW/LMW blends. From these experiments, insights were gained into the processing characteristics of these resins. Of interest, was the frequency dependence of the complex viscosity, the storage and loss modulus. From these dependencies, the shear thinning behavior, zero-shear viscosity, melt elasticity, and melt miscibility of blends were compared.

Figure 5 shows the variation of the complex viscosity (η^*) versus frequency at 190°C for the HMW/LMW blends. Since there are more short molecular chains in LMW than HMW, HMW

Table II. Dynamic Rheological Parameters of the HMW/LMW Blends

HMW/LMW	η_0 (Pa s)	ω_0 (Hz)	m	G_x (Pa)
100/0	1.81×10^6	6.25×10^{-5}	0.692	-
90/10	1.08×10^6	1.22×10^{-4}	0.674	1.89×10^4
80/20	7.93×10^5	1.35×10^{-4}	0.674	1.60×10^4
70/30	4.90×10^5	1.46×10^{-4}	0.633	1.53×10^4
60/40	3.36×10^5	1.83×10^{-4}	0.613	1.10×10^4

exhibits greater viscosity than LMW (which have been omitted because of very low viscosity). All of the blends show an intermediate behaviour and a decrease in η^* can be observed with an increase in the content of LMW. In the low frequency region, the viscosity of a polymer generally approaches a constant value where the viscosity is independent of the frequency, and it is the zero shear viscosity. Using the relation developed by Cox-Merz, the complex viscosity versus frequency can often be interchanged with the shear viscosity versus shear rate. So in order to estimate the zero shear viscosity, the Cross model[16] can be used to adapt to frequency dependent of complex viscosity data:

$$\eta = \eta_0[(1 + |\tau\dot{\gamma}|^m)]^{-1} \quad (1)$$

where η_0 is the zero shear viscosity, τ is the average relaxation time and m is the pesudoplasticity index. The experimental data adjusted to the Cross equation were shown as the solid lines in Figure 5, and the fitted data are listed in Table II.

The correlation between η_0 and M_w is presented in Figure 6, which shows that the data are well adjusted to a straight line. The conventional polyethylene (include bimodal PE) can be well fitted to the equation proposed by Raju et al.[35] at 190°C:

$$\eta_0 = K(M_w)^{3.6} \quad (2)$$

On the other hand, the results of HMW/LMW blends are well adjusted to a power law equation with an exponent of 3.3. This result allows us to state that maybe the HMW/LMW blends

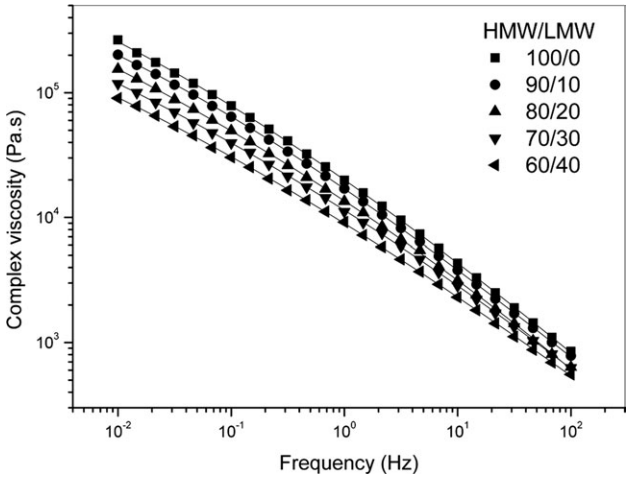

Figure 5. Frequency dependence of η^* for HMW/LMW blends at 190°C (the solid lines represent curve-fitting using Cross model).

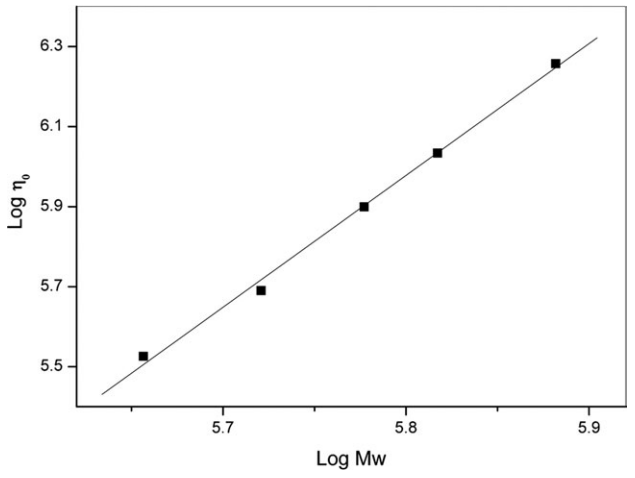

Figure 6. Weight average molecular weight dependence of η^0 for the blends at 190°C.

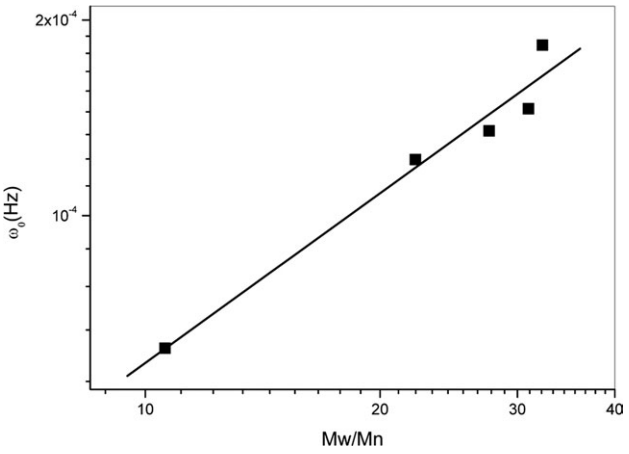

Figure 7. M_w/M_n dependence of ω_0 for the HMW/LMW blends.

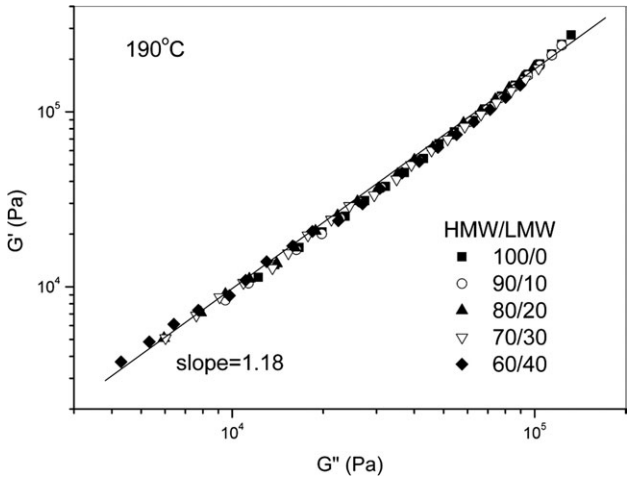

Figure 9. G' versus G'' for HMW/LMW blends at 190°C.

with more distinct bimodal MWD characteristic than that of commercial bimodal polyethylenes, which give rise to considerably lower viscosities. The zero-shear viscosity is a reflection of the polymer chain entanglements, and LMW with shorter molecular chains may reduce the total entanglement density of HMW/LMW blends.

The onset of frequency dependency of viscosity (non-Newtonian, shear thinning behavior) can be defined as a characteristic frequency (ω_0). The values of ω_0 defined as $\eta(\omega_0) = 0.8\eta_0$[36] are presented in Table II. Because of the practical importance of shear thinning behavior in polymer melt rheology, the correlation between ω_0 and polydispersity index is established, and the data is well fitted to a straight line (Figure 7) with a equation of $\omega_0 = 8.05 \times 10^{-6}(M_w/M_n)^{0.86}$. The values of ω_0 increase and values of m (Table II) decrease with increasing in the content of LMW, indicating that LMW recedes the pesudoplasticity (shear thinning) of the blends because that the shorter molecular chains can play a dilution effect between the longer molecular chains and weaken the chain entanglements.

The log-additivity rule based on the zero-shear viscosity or complex viscosity is always used to investigate the miscibility of polymer blends. For log-additive component plots, partially miscible or immiscible blends exhibit positive or negative deviation from linearity owing to the phase morphologies.[37,38] The component dependence on the complex viscosity η^* at different frequencies for the HMW/LMW blends are plotted in Figure 8 form data obtained at 190°C, which shows that the HMW/LMW blends almost perfectly follow the log-additivity rule, suggesting the miscibility of the blends. Similar results obtained for the blends at other temperature are not presented here.

Han-plots, defined as G' versus G'' in logarithmic scale proposed by Han et al.[39] are compared with further investigate the miscibility of polymer blends. For the homogeneous polymer system, Han-plots are independent on either component or temperature. Figure 9 shows the Han-plots of the HMW/LMW blends form data obtained at 190°C. As shown, G' versus G'' of the blends exhibit single-phase behavior since all the plots are generally linear with the same slope of about 1.18, and the regions of the blends properties overlap that of the pure HMW and LMW. The Han-plots for every sample were also obtained at different temperature, 150, 170, 190, and 210°C, and the

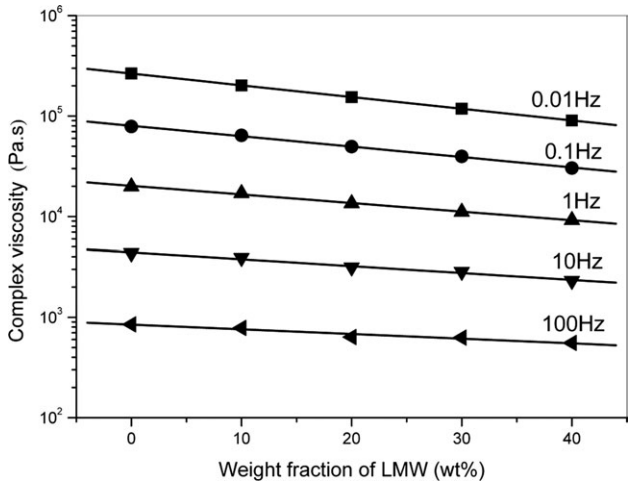

Figure 8. Log additivity of viscosity and blend composition at 190°C.

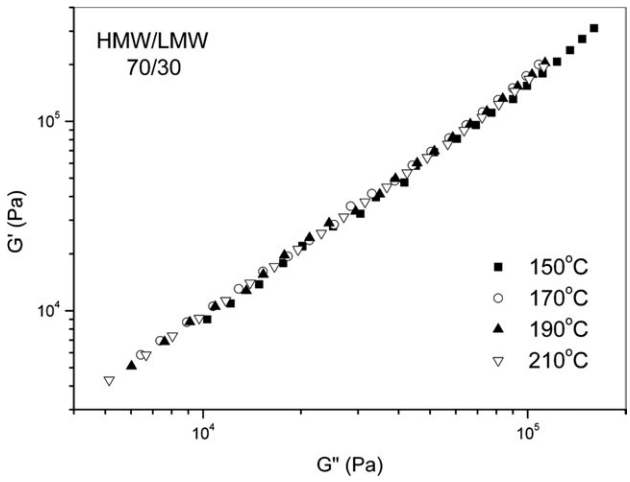

Figure 10. Han-plots of the HMW/LMW blend with 30 wt % LMW at different temperature.

results for the HMW/LMW blend with 30 wt % LMW are plotted in Figure 10 (the rest have been omitted to avoid crowding). As can be seen in Figure 10, all the plots are also generally linear and have the almost completely same slope. Thus, it is believed that HMW and LMW is melt miscible for these blends.

Data of storage and loss modulus for the HMW/LMW blend with 30 wt % LMW are shown in Figure 11 referred to 190°C, and the time-temperature superposition (TTS) principle was introduced to certificate the thermorheological simplicity of the blend in melt state. Similar trends obtained for the other blends are not presented here. As shown in Figure 11, the TTS principle works well, and excellent superposition for both G' and G'' was obtained, suggesting the thermorheological simplicity in accordance with the results of Han-plots. Moreover, from the plots as those displayed in Figure 11 the dynamic cross-point defined as $G_x = G'' = G'$ can be determined. Cross-point values, which in fact separate viscous-like and elastic-like behaviors, are include in Table II. These values, as well as G_x values are plotted as a function of polydispersity index in Figure 12, where we observe that G_x decreases as polydispersity index increasing, and follows a power-law equation with an exponent of −1.14.

CONCLUSIONS

Polyethylene blends with distinct bimodal MWD were successfully prepared via blending HMW with LMW. The thermal and rheological properties of the HMW/LMW blends were investigated by DSC and dynamic rheological measurements. The main features of these blends were the following:

1. From the thermal analysis, cocrystallization of HMW and LMW took place, indicating the HMW/LMW blends were miscible in the crystalline state. Based on the log-additivity rule for complex viscosity and the features of Han-plots, the HMW/LMW blends were believed to be miscible in the melt state.

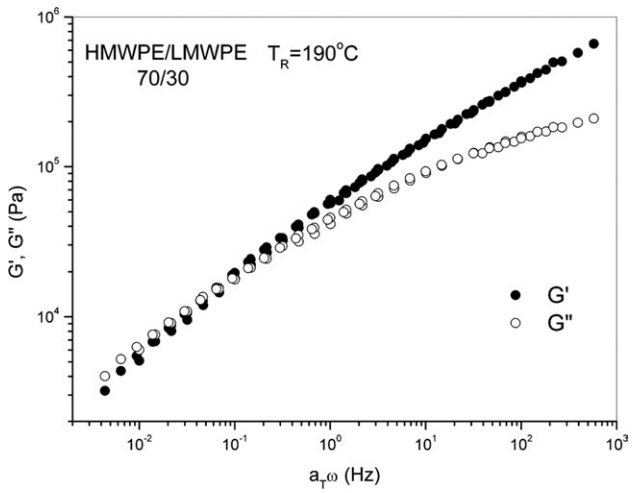

Figure 11. Time-temperature superposition of storage and loss modulus for the HMW/LMW blend with 30 wt % at the reference temperature of 190°C.

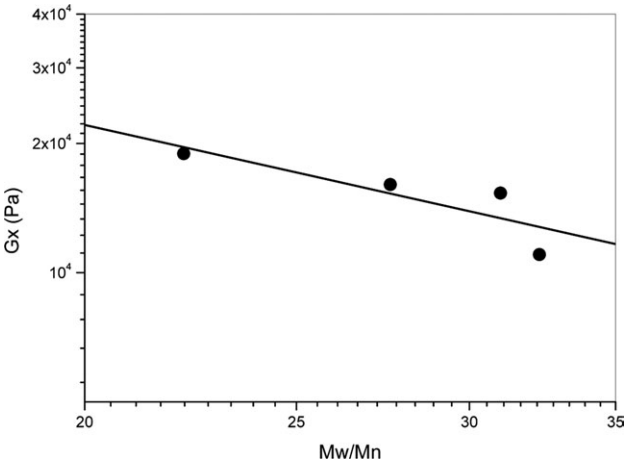

Figure 12. Cross-point modulus vs polydispersity index for the HMW/LMW blends.

2. In the case of HMW/LMW blends, an exponent of 3.3 was found for a power law equation of η_0 (190°C) versus M_w, instead of the exponent 3.6 found for conventional polyethylene.
3. The correlations between ω_0 and polydispersity index, and between G_x and polydispersity index were established and fitted to the power law equation with an exponent of 0.86 and −1.14, respectively.

ACKNOWLEDGMENTS

The authors gratefully appreciate the financial support for this work by National Natural Science Foundation of China (51073109).

REFERENCES

1. Archie, E. H.; Soares, J. B. P. *Prog. Polym. Sci.* **1996**, *21*, 651.
2. Brichinger, H. H.; Waymouth, R. M. *Angew. Chem. Int. Ed. Engl.* **1995**, *34*, 1143.
3. Vega, J. F.; Munoz-Escalona, A.; Santamaria, A. *Macromolecules* **1996**, *29*, 960.
4. Munoz-Escalona, A.; Lafuente, P.; Vega, J. F.; Santamaria, A. *Polym. Eng. Sci.* **1999**, *39*, 2292.
5. Alt, F. P.; Bohm, L. L.; Enderle, H. F. *Symposia* **2001**, *163*, 135.
6. Markus, G. *Prog. Polym. Sci.* **2001**, *26*, 895.
7. Liu, C. Y.; Wang, J.; He, J. S. *Polymer* **2002**, *43*, 3811.
8. Bohm, L. L. *Angew. Chem. Int. Ed. Engl.* **2003**, *42*, 5010.
9. Galli, P.; Vecellio, G. *Prog. Polym. Sci.* **2001**, *26*, 1287.
10. Scheirs, J.; Bohm, L. L.; Leevers, P. S. *Trends Polym. Sci.* **1996**, *4*, 408.
11. Liu, H. T.; Davey, C.R.; Shirodkar, P. P. *Macromol. Symp.* **2003**, *195*, 309.
12. Yang, L.; Somani, R. H.; Sics, I.; Hsiao, B. S.; Kolb, R. *Macromolecules* **2004**, *37*, 4845.
13. Zuo, F.; Keum, J. K.; Yang, L.; Somani, R. H.; Hsiao, B. S. *Macromolecules* **2006**, *39*, 2209.

14. Krumme, A.; Lehtinen, A.; Viikna, A. *Eur. Polym. J.* **2004**, *40*, 359.
15. Krumme, A.; Lehtinen, A.; Viikna, A. *Eur. Polym. J.* **2004**, *40*, 371.
16. Dealy, M.; Wissbrun, K. F. Melt rheology and Its Role in Plastics Processing: Theory and Applications; New York: Van Nostrand Reinhold, **1990**; Chapters 4, 10.
17. Mavridis, H.; Shroff, R. *J. Appl. Polym. Sci.* **1993**, *49*, 299.
18. Wood-Adams, P. M.; Dealy, J. M.; Degroot, A. W. *Macromolecules* **2000**, *33*, 7489.
19. Kzatchkov, I. B.; Bohnet, N.; Goyal, S. K.; Hazikiriakos, S. G. *Polym. Eng. Sci.* **1999**, *39*, 804.
20. Kim, Y. S.; Chung, C. I.; Lai, S. Y.; Hyun, K. S. *J. Appl. Polym. Sci.* **1996**, *59*, 125.
21. Vega, J. F.; Santamaria, A.; Munoz-Escalona, A. *Macromolecules* **1998**, *31*, 3639.
22. Vega, J. F.; Fernandez, M.; Santamaria, A.; Munoz-Escalona, A.; Lafuente, P. *Macromol. Chem. Phys.* **1999**, *200*, 2257.
23. Hatzikiriakos, S. G. *Polym. Eng. Sci.* **2000**, *40*, 2279.
24. Goyal, S. K.; SPE Antec'94 Conference Proceedings **1994**, p 1232.
25. Foster, G. N.; Wasserman, S. H. Metcon, Houston, TX, **1997**.
26. DesLauriers, P. J.; McDaniel, M. P.; Rohlfing, D. C.; Krishnaswamy, R. K.; Secora, S. J.; Benham, E. A. *Polym. Eng. Sci.* **2005**, *45*, 1203.
27. Hong-Wang, S.; Bang-Hu, X.; Wei, Y.; Ming-Bo, Y. *J. Appl. Polym. Sci.* **2011**, *121*, 1543.
28. Xin, S.; Hong-wang, S.; Bang-Hu, X.; Wei, Y.; Ming-Bo, Y. *Polymer* **2011**, *52*, 564.
29. Quan-Bing, W.; Bang-Hu, X.; Wei, Y.; Ming-Bo, Y. *J. Macromol. Sci. Pure Appl. Chem.* **2010** *47*, 1123.
30. Shan, C. L. P.; Joao, B. P.; Penlideis, A. *Polymer* **2002**, *43*, 7345.
31. Shan, C. L. P.; Joao, B. P.; Penlideis, A. *Polymer* **2003**, *44*, 177.
32. Gottfried, W. E. Polymer Materials: Structure-Properties-Applications; Carl Hanser Verlag: Munich, **2001**; Chapters 4, 48.
33. Arnal, M. L.; Sancgez, J. J.; Muller, A. J. *Polymer* **2001**, *42*, 6877.
34. Rana, D.; Lee, C. H.; Cho, K.; Lee, B. H.; Choe, S. *J. Appl. Polym. Sci.* **1998**, *69*, 2441.
35. Raju, V. R.; Smith, G. G.; Marin, G.; Knox, J. R.; Graessley, W. W. *J. Polym. Sci.: Polym. Phys. Ed.* **1979**, *17*, 1183.
36. Graessley, W. W. *Adv. Polym. Sci.* **1974**, *16*, 1.
37. Cho, K.; Lee, B. H.; Hwang, K. M.; Lee, H.; Choe, S. *Polym. Eng. Sci.* **1998**, *38*, 1969.
38. Xanthos, M.; Tan, V.; Ponnusamy, A. *Polym. Eng. Sci.* **1997**, *37*, 1102.
39. Han, C. D.; Lem, K. W. *Polym. Eng. Rev.* **1982**, *2*, 135.